High harmonic generation from an atom in a squeezed-vacuum environment

ShiJun Wang,[1,2] ShaoGang Yu,[1] XuanYang Lai,[1,3,*] and XiaoJun Liu[1,†]

[1]*State Key Laboratory of Magnetic Resonance and Atomic and Molecular Physics, Wuhan Institute of Physics and Mathematics, Innovation Academy for Precision Measurement Science and Technology, Chinese Academy of Sciences, Wuhan 430071, China*

[2]*School of Physical Sciences, University of Chinese Academy of Sciences, Beijing 100049, China*

[3]*Wuhan Institute of Quantum Technology, Wuhan 430206, China*

(Received 12 June 2023; revised 25 March 2024; accepted 5 June 2024; published 1 July 2024)

We investigate high harmonic generation (HHG) of an atom in the presence of squeezed vacuum of a single harmonic mode. Based on a fully quantum time-dependent Schrödinger equation, we derive an analytical formula for the harmonic amplitude. Our simulations of the HHG spectrum with this formula show that the harmonic amplitude of the corresponding squeezed mode can undergo significant changes with different parameters of the squeezed vacuum. Using the time-frequency analysis method, the physics underlying the effects of the vacuum quantum fluctuation (VQF) on the harmonic generation is revealed, which is found to be consistent with the explanation of Fermi's golden rule. Our work establishes a profound connection between harmonic generation and VQF, and may provide an unconventional approach to manipulating harmonic emission.

DOI: 10.1103/PhysRevResearch.6.033010

I. INTRODUCTION

High harmonic generation (HHG) is an intriguing nonlinear optical phenomenon that occurs during intense laser-atom interactions [1,2]. Over the past three decades, HHG has attracted considerable attention for its wide range of applications, including table-top coherent XUV generation [3,4], molecular orbital imaging [5,6], and attosecond science [7,8]. Usually, the study of HHG has focused primarily on the laser-induced dipole moment of the atom from the perspective of classical electrodynamics [9–11]. Recently, there has been a growing interest in a quantized description of HHG and the driving lights based on the theory of quantum electrodynamics (QED) [12–21], which opens the way for generation of high-intensity quantum light states.

It is worth noting that in QED theory, photon emission from electronic transitions in an atom is also affected by vacuum quantum fluctuation (VQF) of the corresponding emission mode [22]. This aspect of QED has been instrumental in explaining a variety of fundamental phenomena, such as spontaneous emission [22]. Furthermore, based on this effect, VQF has been shown to effectively control quantum processes [23]. For example, by manipulating VQF with photonic crystals, the spontaneous emission rate of an atom inside the photonic crystals can be controlled [24]. Similarly, for the HHG process, the emission of harmonic photons also originates from the electron transition during the electron recombination with the atomic core [25,26]. However, whether the harmonic emission is influenced by VQF of the corresponding harmonic mode remains unknown.

In QED theory, the vacuum state of the harmonic mode is usually described with a coherent state characterized by a constant fluctuation [27]. To study the effect of VQF of the harmonic mode on HHG, it is necessary to use a vacuum state with controllable fluctuations in the time domain, i.e., a squeezed vacuum state [28,29]. Currently, various experimental techniques have been developed to generate these squeezed vacuum states, including the optical parametric amplification process involving the interaction of a frequency-doubled continuous pump light with a second-order nonlinear crystal [30,31], as well as the four-wave mixing process employing the third-order nonlinear effect of an atomic ensemble [32,33]. A recent experiment with the optical parametric amplification method has successfully achieved a squeezed vacuum state with a squeezing parameter of $r = 1.74$ [34]. In addition, the generated squeezed vacuum state with these techniques is usually in the near-infrared (NIR) or mid-infrared (mid-IR) region. Recently, a quantum frequency up-conversion method has been developed and experimentally demonstrated to generate the squeezed vacuum in the visible region [35,36]. These advances in squeezed vacuum generation provide opportunities to study the influence of VQF of the harmonic mode on the corresponding harmonic emission.

In this work, we study HHG from intense laser-atom interaction in a squeezed vacuum of the harmonic mode. Taking into account the practical experimental conditions, we consider only a single-mode squeezed vacuum. Based on a fully quantum time-dependent Schrödinger equation (TDSE), an analytical formula of the harmonic amplitude in the presence of the single-mode squeezed vacuum is derived. Our simulations of the HHG spectra with this formula show that

*Contact author: xylai@wipm.ac.cn
†Contact author: xjliu@wipm.ac.cn

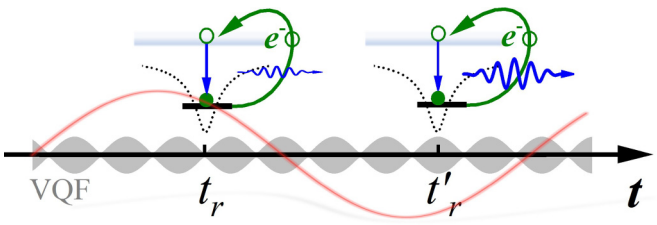

FIG. 1. Schematic view of HHG from intense laser-atom interaction in a squeezed vacuum of a harmonic mode. The motion of an electron in a strong driving laser field (red curve) is depicted by the green curve [25,26], and the emission of harmonics resulting from the electron's transition back to the atomic core is represented by the blue curve. Due to the influence of the quantum fluctuation of the squeezed vacuum (gray shadow) on the electron transition probability, the harmonic amplitude of the corresponding squeezed mode emitted at time t_r is weak but becomes strong at t'_r.

the harmonic amplitude of the corresponding squeezed mode is changed with the quantum fluctuation of the squeezed vacuum. Using the time-frequency analysis method, we reveal that the effect of VQF is due to the influence of the squeezed vacuum on the probability of the electron transition. Thus, the corresponding harmonic amplitude is affected accordingly (as shown in Fig. 1). Our result is in good agreement with the explanation of Fermi's golden rule [22]. The close relationship between HHG and VQF, as revealed in our work, may provide an approach to control the harmonic generation.

This article is organized as follows. In Sec. II, we briefly introduce the theoretical method for HHG from intense laser-atom interaction in a squeezed vacuum of a single harmonic mode. In Sec. III, we present the simulated HHG spectra under different squeezed vacuum states. Subsequently, we reveal the underlying physics for the influence of the squeezed vacuum on HHG. Finally, our conclusions are given in Sec. IV. Throughout this article, atomic units (a.u.) are used unless explicitly stated otherwise.

II. THEORETICAL METHOD

We start from the fully quantum TDSE based on the QED theory for a strong laser-atom interaction [27]

$$i\frac{\partial}{\partial t}|\Psi(t)\rangle = [\hat{H}_0 - \mathbf{r}\cdot\hat{\mathbf{E}} + \hat{H}_f]|\Psi(t)\rangle, \tag{1}$$

where $\hat{H}_0 = \mathbf{p}^2/2 + U(\mathbf{r})$ is the Hamiltonian of the atomic system with the kinetic term $\mathbf{p}^2/2$ and the Coulomb potential $U(\mathbf{r})$. $\hat{H}_f = \sum_{\mathbf{k}} \omega_{\mathbf{k}} \hat{a}^\dagger_{\mathbf{k}} \hat{a}_{\mathbf{k}}$ describes the Hamiltonian of the electromagnetic field, which contains all the frequency modes $\omega_{\mathbf{k}}$ with the creation operator $\hat{a}^\dagger_{\mathbf{k}}$ and the annihilation operator $\hat{a}_{\mathbf{k}}$, and $-\mathbf{r}\cdot\hat{\mathbf{E}}$ is the interaction term in the dipole approximation with the quantized electromagnetic field $\hat{\mathbf{E}} = i\sum_{\mathbf{k}} \sqrt{\frac{\omega_{\mathbf{k}}}{2V}}(\hat{a}_{\mathbf{k}} - \hat{a}^\dagger_{\mathbf{k}})$ and the normalization volume V. The initial state of the atom and the electromagnetic fields is expressed as $|\Psi(-\infty)\rangle = |\phi_i\rangle \otimes |\alpha_{\mathbf{k}_0}, \xi_{\mathbf{k}_0}\rangle \otimes \prod_{\mathbf{k}} |0_{\mathbf{k}}, \xi_{\mathbf{k}}\rangle$. Here, $|\phi_i\rangle$ represents the ground state of the atom, $|\alpha_{\mathbf{k}_0}, \xi_{\mathbf{k}_0}\rangle$ denotes the driving light, and $\prod_{\mathbf{k}} |0_{\mathbf{k}}, \xi_{\mathbf{k}}\rangle$ represents the vacuum state of the harmonic modes. The parameter $\xi_{\mathbf{k}}$ $(= r_{\mathbf{k}} e^{i\theta_{\mathbf{k}}})$ describes the squeezing of the vacuum with the squeezing parameter $r_{\mathbf{k}}$ and the squeezing angle $\theta_{\mathbf{k}}$ [27,29]. For the single-mode squeezed vacuum state, if $\xi_{\mathbf{k}_s} = \xi$ for a given mode $\mathbf{k}_s$ (including $\mathbf{k}_0$), then $\xi_{\mathbf{k}} = 0$ (i.e., $r_{\mathbf{k}} = 0$) for all other modes $\mathbf{k} \neq \mathbf{k}_s$.

Next, we derive the harmonic amplitude from Eq. (1). First, the Hamiltonian in Eq. (1) is transformed into the Heisenberg picture with respect to the electromagnetic field Hamiltonian $\hat{H}_f$ with $e^{-i\hat{H}_f t}$. This transformation leads to the time dependence of the quantized electromagnetic field. Second, we perform a unitary transformation to transform the harmonic modes from the squeezed vacuum state into the coherent vacuum states: $|0_{\mathbf{k}}, \xi_{\mathbf{k}}\rangle = \hat{S}(\xi_{\mathbf{k}})|0_{\mathbf{k}}\rangle$, where $\hat{S}(\xi_{\mathbf{k}}) = e^{(\xi^*_{\mathbf{k}}\hat{a}^2_{\mathbf{k}} - \xi_{\mathbf{k}}\hat{a}^{\dagger 2}_{\mathbf{k}})/2}$ is the squeezed operator of the light fields [27,29]. Consequently, the electric field becomes $\prod_{\mathbf{k}} \hat{S}(\xi_{\mathbf{k}})^\dagger \hat{\mathbf{E}}(t) \prod_{\mathbf{k}} \hat{S}(\xi_{\mathbf{k}}) = \hat{\mathbf{E}}_q(t)$, where $\hat{\mathbf{E}}_q(t)$ represents the quantum fluctuating part of the vacuum field: $\hat{\mathbf{E}}_q(t) = -i\sum_{\mathbf{k}} \sqrt{\frac{\omega_{\mathbf{k}}}{2V}}[(\cosh r_{\mathbf{k}} + \sinh r_{\mathbf{k}} e^{-i(2\omega_{\mathbf{k}}t - \theta_{\mathbf{k}})})\hat{a}^\dagger_{\mathbf{k}} e^{i\omega_{\mathbf{k}}t} - (\cosh r_{\mathbf{k}} + \sinh r_{\mathbf{k}} e^{i(2\omega_{\mathbf{k}}t - \theta_{\mathbf{k}})})\hat{a}_{\mathbf{k}} e^{-i\omega_{\mathbf{k}}t}]$. Third, we also perform a unitary transformation to transform the driving field into the coherent vacuum state: $|\alpha_{\mathbf{k}_0}, \xi_{\mathbf{k}_0}\rangle = \hat{D}(\alpha_{\mathbf{k}_0})\hat{S}(\xi_{\mathbf{k}_0})|0_{\mathbf{k}_0}\rangle$, where $\hat{D}(\alpha_{\mathbf{k}_0}) = e^{\alpha_{\mathbf{k}_0}\hat{a}^\dagger_{\mathbf{k}_0} - \alpha^*_{\mathbf{k}_0}\hat{a}_{\mathbf{k}_0}}$ represents Glauber's shift operator [27]. Accordingly, the driving light becomes the superposition of the quantum fluctuation part $\hat{\mathbf{E}}_{q_{\mathbf{k}_0}}(t) = -i\sqrt{\frac{\omega_{\mathbf{k}_0}}{2V}}[(\cosh r_{\mathbf{k}_0} + \sinh r_{\mathbf{k}_0} e^{-i(2\omega_{\mathbf{k}_0}t - \theta_{\mathbf{k}_0})})\hat{a}^\dagger_{\mathbf{k}_0} e^{i\omega_{\mathbf{k}_0}t} - (\cosh r_{\mathbf{k}_0} + \sinh r_{\mathbf{k}_0} e^{i(2\omega_{\mathbf{k}_0}t - \theta_{\mathbf{k}_0})})\hat{a}_{\mathbf{k}_0} e^{-i\omega_{\mathbf{k}_0}t}]$ and the classical field part $\mathbf{E}_c(t) = i\sqrt{\frac{\omega_{\mathbf{k}_0}}{2V}}(\alpha_{\mathbf{k}_0} e^{-i\omega_{\mathbf{k}_0}t} - \alpha^*_{\mathbf{k}_0} e^{i\omega_{\mathbf{k}_0}t})$. Therefore, Eq. (1) can be rewritten as

$$i\frac{\partial}{\partial t}|\psi(t)\rangle = [\hat{H}_c - \mathbf{r}\cdot\hat{\mathbf{E}}_Q(t)]|\psi(t)\rangle, \tag{2}$$

where $\hat{H}_c = \hat{H}_0 - \mathbf{r}\cdot\mathbf{E}_c(t)$, corresponding to the Hamiltonian of an atom in the classical part $\mathbf{E}_c(t)$ of the driving laser field, and $\hat{\mathbf{E}}_Q$ denotes quantum fluctuations of all the frequency modes.

After that, we use the interaction picture with respect to $\hat{H}_c$ to solve the TDSE in Eq. (2). For the squeezed vacuum with small squeezing parameter, the quantum fluctuation part is typically weak, and thus we can approximately solve the TDSE by expanding the time-ordered exponential to the first order [13]. Accordingly, the TDSE solution can be expressed as

$$|\psi(t)\rangle \doteq |\phi_i(t)\rangle|0\rangle + \sum_j \sum_{\mathbf{k}} \sqrt{\frac{\omega_{\mathbf{k}}}{2V}} \left[\int_{-\infty}^{t} \mu_{\mathbf{k}}(\tau)\mathbf{d}_{ji}(\tau)e^{i\omega_{\mathbf{k}}\tau}d\tau\right] |\phi_j(t)\rangle|1_{\mathbf{k}}\rangle, \tag{3}$$

where $|\phi_j(t)\rangle$ is the time-dependent electron wavefunction, evolving from an eigenstate ϕ_j of the atom under the Hamiltonian of $\hat{H}_c$, $\mathbf{d}_{ji}(\tau) = \langle\phi_j(\tau)|\mathbf{z}|\phi_i(\tau)\rangle$ is the dipole matrix elements for the linearly polarized laser field, and $|1_{\mathbf{k}}\rangle = \hat{a}^\dagger_{\mathbf{k}}|0\rangle$ denotes the generation of one harmonic photon from the vacuum state with a mode of $\mathbf{k}$. The time-dependent term $\mu_{\mathbf{k}}(t)$ comes from the quantum fluctuation part with $\hat{a}^\dagger_{\mathbf{k}}$:

$$\mu_{\mathbf{k}}(t) \equiv \cosh r_{\mathbf{k}} + \sinh r_{\mathbf{k}} e^{-i(2\omega_{\mathbf{k}}t - \theta_{\mathbf{k}})}, \tag{4}$$

which is closely related to the magnitude of VQF of a mode $\mathbf{k}$. It is worth noting that, when $j = i$ in Eq. (3), $\mathbf{d}_{ii}(\tau)$ is the

conventional laser-induced dipole matrix element and the Fourier transform of the dipole moment $\mathbf{d}_{ii}(\tau)$ corresponds to the harmonic amplitude in the traditional HHG theory, whereas $\mathbf{d}_{ji}(\tau)$ with $j \neq i$ is the correction term. It has been shown [13] that the contribution of the conventional element $\mathbf{d}_{ii}(\tau)$ is typically dominant for HHG in the current experimental measurement. Therefore, for simplicity, we mainly focus on the contribution of the term $\mathbf{d}_{ii}(\tau)$ in our work.

Furthermore, we calculate the total energy of the emitting harmonics using Eq. (3) to obtain the expression for the emission per unit frequency [13]. The corresponding harmonic spectrum of the emitting field is given by

$$P(\omega_{\mathbf{k}}) = \frac{\omega_{\mathbf{k}}^4}{6\pi^2 c^3}\left|\int_{-\infty}^{\infty} \mu_{\mathbf{k}}(\tau)\mathbf{d}_{ii}(\tau)e^{i\omega_{\mathbf{k}}\tau}d\tau\right|^2. \quad (5)$$

In this work, we simulate the HHG spectra according to Eq. (5). For simplicity, a one-dimensional model atom with the soft Coulomb potential $U(x) = -1/\sqrt{x^2 + s_c}$ is used in our simulation. When the soft-core parameter $s_c = 1.41$, the ionization potential of the atom is approximately 15.8 eV, which matches the ground state of the Ar (argon) atom.

III. RESULTS AND DISCUSSION

According to Eq. (5), we simulate the HHG spectra of an atom in the presence of a squeezed vacuum of, e.g., the first-order harmonic mode and the ninth-order harmonic mode, respectively. Note that the current squeezed vacuum can only be generated in the mid-IR, NIR, and visible regions [35,36]. Considering the realistic scenario, when studying the effect of the first-order squeezed mode, we can use the driving light with a wavelength of, e.g., 800 nm, whereas when studying the effect of the ninth-order squeezed mode, the driving light with a longer wavelength of, e.g., 3600 nm is used. In Figs. 2(a) and 2(b), we show the simulated HHG spectra in the first-order harmonic mode with $\theta_{\mathbf{k}} = 0.9\pi$ and the ninth-order harmonic mode with $\theta_{\mathbf{k}} = 0.27\pi$, respectively, as a function of squeezing parameter $r_{\mathbf{k}}$. In practice, adjusting the squeezing parameter and squeezing angle of the single-mode squeezed vacuum can be realized by changing the pump power and tuning the relative phase between seed wave and pump wave [34,37]. Our simulation shows that with the increase of the value of $r_{\mathbf{k}}$, the amplitude of the first-order harmonic in Fig. 2(a) and the ninth-order harmonic in Fig. 2(b) is changed significantly, whereas the amplitudes of other harmonics remain the same. Furthermore, in Figs. 2(c) and 2(d), we show the amplitude of the first- and ninth-order harmonics in the corresponding single-mode squeezed vacuum with different $r_{\mathbf{k}}$ as a function of $\theta_{\mathbf{k}}$. It is found that the harmonic amplitude also changes with the squeezing angle and the maximum amplitude of the harmonic increases with the increase of $r_{\mathbf{k}}$, exceeding an order of magnitude at $r_{\mathbf{k}} = 1.5$. Therefore, our result shows that the harmonic amplitude is affected by the corresponding squeezed vacuum. Note that the squeezing parameter of the squeezed vacuum state we used is small, which is different from that used in previous works [17,18]. In the following, we will understand the impact of the squeezed vacuum on the harmonic emission.

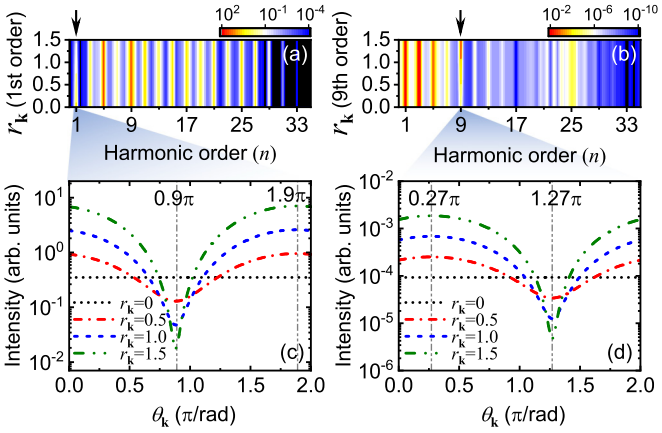

FIG. 2. (a), (b) TDSE simulations of the HHG spectra of an atom in a squeezed vacuum of the first-order harmonic mode with the squeezing angle $\theta_{\mathbf{k}} = 0.9\pi$ and the ninth-order harmonic mode with $\theta_{\mathbf{k}} = 0.27\pi$, respectively, as a function of the squeezing parameter $r_{\mathbf{k}}$. Considering a realistic scenario, the wavelengths of the driving light are 800 nm and 3600 nm, respectively. For more details, see the text. In (b), to better illustrate the change of the amplitude of the ninth-order harmonic, only a part of the harmonic orders are shown. (c) and (d) The amplitude of the first- and ninth-order harmonics in the corresponding single-mode squeezed vacuum state with different $r_{\mathbf{k}}$ as a function of $\theta_{\mathbf{k}}$. In our simulation, the driving light has a peak intensity of $I = 1.15 \times 10^{14}\,\mathrm{W/cm^2}$ with a trapezoidal profile (up- and down-ramped over two cycles, constant over six cycles).

First, we analyze the derived formula for the harmonic amplitude in Eq. (5). Different from the conventional strong-field theory of HHG [38,39], there is an additional term $\mu_{\mathbf{k}}(t)$ in the integral, which is related to the magnitude of VQF of the mode $\mathbf{k}$. Thus, the corresponding harmonic amplitude is influenced not only by the dipole moment but also by VQF. Moreover, since the term $\mu_{\mathbf{k}}(t)$ is the function of $r_{\mathbf{k}}$ and $\theta_{\mathbf{k}}$ according to Eq. (4), the harmonic amplitude varies with different squeezed vacuum states, as shown in Fig. 2. In contrast, for other modes with $r_{\mathbf{k}} = 0$, the term $\mu_{\mathbf{k}}(t) = 1$, and thus Eq. (5) can be simplified to the formula used in conventional HHG theory.

To get a deep insight into the underlying physics for the effect of VQF on HHG, we perform the time-frequency analysis of the resulting HHG using wavelet transform [40]. The corresponding expression for the transform is given by

$$A(\omega_{\mathbf{k}}, t) = \int \mu_{\mathbf{k}}(t')\mathbf{d}_{ii}(t')\sqrt{\omega_{\mathbf{k}}}W[\omega_{\mathbf{k}}(t' - t)]dt', \quad (6)$$

where $W(x) = \frac{1}{\sqrt{\tau}}e^{ix}e^{-x^2/2\tau^2}$ represents the mother wavelet [41]. This wavelet time-frequency profile of HHG provides insight into the emission of harmonics resulting from the transition of the returned electron in the time domain [40]. In Figs. 3(a) and 3(b), we present the wavelet time-frequency profile of the first-order harmonic under the squeezed vacuum of the mode $\mathbf{k}_0$ with the squeezing parameter $r_{\mathbf{k}_0} = 0$ (solid black curve) and $r_{\mathbf{k}_0} = 0.5$ (dashed red curve) for the squeezing angles $\theta_{\mathbf{k}_0} = 0.9\pi$ and $\theta_{\mathbf{k}_0} = 1.9\pi$, respectively. The different curves oscillate with a period of $T/2$ [42], where T represents an optical cycle of the driving laser field. A closer inspection reveals that for $\theta_{\mathbf{k}_0} = 0.9\pi$ in Fig. 3(a), the curve with $r_{\mathbf{k}_0} = 0.5$ shows a noticeable time shift compared to that

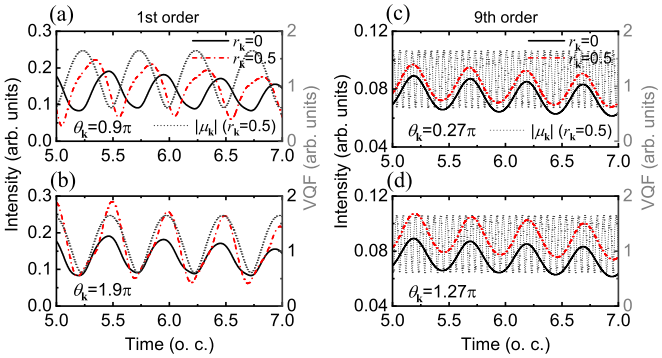

FIG. 3. The wavelet time-frequency profile of the harmonic of the corresponding squeezed mode with $r_{\mathbf{k}} = 0$ (solid black curve) and $r_{\mathbf{k}} = 0.5$ (dashed red curve). The gray dashed curves with respect to the right axis denote the $|\mu_{\mathbf{k}}(t)|$ of the squeezed mode. (a) and (b) present the squeezed vacuum of the first-order harmonic mode with $\theta_{\mathbf{k}} = 0.9\pi$ and 1.9π, respectively. (c) and (d) present the squeezed vacuum of the ninth-order harmonic mode with $\theta_{\mathbf{k}} = 0.27\pi$ and 1.27π, respectively.

of $r_{\mathbf{k}_0} = 0$. Conversely, for $\theta_{\mathbf{k}_0} = 1.9\pi$ in Fig. 3(b), the two curves are nearly in phase, and furthermore, the maximum amplitude increases significantly with $r_{\mathbf{k}_0}$, which is consistent with the TDSE simulation in Fig. 2(c).

The dependence of the wavelet time-frequency profiles on the single-mode squeezed vacuum can be understood qualitatively after making a transformation of Eq. (6). The mother wavelet $W(x)$ in Eq. (6) has a narrow distribution around time t, and the term $\mu_{\mathbf{k}_0}(t)$ changes relatively slowly with respect to time for the mode $\mathbf{k}_0$ [see the gray curve in Fig. 3(a)]. Thus, Eq. (6) can be written approximately as $A(\omega_{\mathbf{k}_0}, t) \sim \int \mathbf{d}_{ii}(t')\sqrt{\omega_{\mathbf{k}_0}} W[\omega_{\mathbf{k}_0}(t'-t)]dt' \times \mu_{\mathbf{k}_0}(t)$. Therefore,

$$\left|A(\omega_{\mathbf{k}_0}, t)\right|^2 \sim \left|\int \mathbf{d}_{ii}(t')\sqrt{\omega_{\mathbf{k}_0}} W\left[\omega_{\mathbf{k}_0}(t'-t)\right]dt'\right|^2 \times \left|\mu_{\mathbf{k}_0}(t)\right|^2, \tag{7}$$

where the term in the first bracket represents the dipole momentum emission of the mode $\mathbf{k}_0$ at time t and the term $|\mu_{\mathbf{k}_0}(t)|^2$ denotes the magnitude of VQF of mode $\mathbf{k}_0$. Fig. 3(a) shows that at $\theta_{\mathbf{k}_0} = 0.9\pi$, there is a noticeable time shift between the curve of the dipole moment emission (solid black curve) and the curve of $|\mu_{\mathbf{k}_0}(t)|$ (gray dashed curve). Thus, the multiplication of the two terms leads to the time shift of the curve of $|A(\omega, t)|^2$ at different $r_{\mathbf{k}_0}$. In contrast, when $\theta_{\mathbf{k}_0} = 1.9\pi$ in Fig. 3(b), the curves of the two terms are in phase. The multiplication of the two terms preserves the phase of the wavelet time-frequency profile and also significantly increases its maximum amplitude.

Notably, physically, the dipole momentum emission in Eq. (7) corresponds to the transition matrix element of the electron between two atomic states with an energy difference of $\omega_{\mathbf{k}_0}$, and the obtained harmonic amplitude denotes the probability of the electron transition. Therefore, our results indicate that the electron transition probability during the electron recombination with the atomic core is influenced by both the transition matrix element of the electron and VQF of the corresponding harmonic mode. This is consistent with the explanation provided by Fermi's golden rule [22] that the probability of electron transition $\mathscr{P}_{fi} \propto |\langle f|\hat{H}|i\rangle|^2\rho$, where $\langle f|\hat{H}|i\rangle$ represents the matrix element between the various energy eigenstates of a quantum system, and ρ is the density of photonic states and quantifies the magnitude of VQF for photon emission [43].

Similarly, we also present the wavelet time-frequency profile of the ninth-order harmonic under the squeezed vacuum of the corresponding harmonic mode with $\theta_{\mathbf{k}} = 0.27\pi$ and $\theta_{\mathbf{k}} = 1.27\pi$ in Figs. 3(c) and 3(d), respectively. Different from the first-order harmonic, the wavelet time-frequency profile at $r_{\mathbf{k}} = 0.5$ is always larger than that at $r_{\mathbf{k}} = 0$ for different squeezing angles. This result can also be understood after making a transformation of Eq. (6). For the ninth-order harmonic, the curve related to VQF oscillates much faster than that of the dipole moment emission [see the gray dashed curves in Figs. 3(c) and 3(d)]. By employing the average value method within the high-frequency approximation, Eq. (6) can be approximated as $A(\omega_{\mathbf{k}}, t) \sim \int \bar{\mu}_{\mathbf{k}}\mathbf{d}_{ii}(t')\sqrt{\omega_{\mathbf{k}}} W[\omega_{\mathbf{k}}(t'-t)]dt'$, where $\bar{\mu}_{\mathbf{k}}$ is the average value of the high-frequency oscillatory term $\mu_{\mathbf{k}}(t)$ over one oscillation period. In this case, the amplitude of the harmonic emission can be approximately written as

$$|A(\omega_{\mathbf{k}}, t)|^2 \sim \left|\int \mathbf{d}_{ii}(t')\sqrt{\omega_{\mathbf{k}}} W[\omega_{\mathbf{k}}(t'-t)]dt'\right|^2 \times |\bar{\mu}_{\mathbf{k}}|^2. \tag{8}$$

Different from first-order harmonic in Eq. (7), the term $|\bar{\mu}_{\mathbf{k}}|^2$ is time independent, and it can be easily seen from Eq. (4) that the value of $|\bar{\mu}_{\mathbf{k}}|^2$ exceeds unity for $r_{\mathbf{k}} > 0$. Therefore, the amplitude of the ninth harmonic increases in the squeezed vacuum, which is consistent with the observation from Figs. 3(c) and 3(d). Our explanation based on Eq. (8) is also in agreement with the explanation of Fermi's golden rule.

It is worth noting that in Fig. 2(d), the ninth-order harmonic amplitude in the HHG spectrum shows a significant change with the squeezing angle $\theta_{\mathbf{k}}$, which is different from the result shown in Figs. 3(c) and 3(d). This is ascribed to Fig. 2(d) being calculated from Eq. (5), whereas Figs. 3(c) and 3(d) are calculated from Eq. (6). In Eq. (6), there is an additional term e^{-x^2/τ^2} with a narrow temporal distribution, which makes the integration only over small region of the time. In contrast, the integration in Eq. (5) is over all times, which physically indicates that the harmonics from different times interfere with each other constructively or destructively. Furthermore, the value of $\mu_{\mathbf{k}}(t)$ in Eq. (5) is complex and is a function of the squeezing angle according to Eq. (4), leading to the final harmonic amplitude changing with the squeezing angle. By using this particular relationship between the harmonic amplitude and the squeezing angle, one can improve the conversion efficiency of HHG, and additionally, it is possible to fit the time-dependent dipole moment according to Eq. (5), which is closely related to the electron wavefunction and thus encodes rich information about electron dynamics.

Finally, we propose an experimental scheme to show the influence of the quantum fluctuation of a single-mode squeezed vacuum on harmonic emission. Currently, the squeezed vacuum can be generated in the mid-IR, IR, and visible regions [35,36]. Thus, in principle, we can control the squeezed vacuum environment around the atom in

experiments to affect the corresponding harmonic amplitude during the HHG process. For the first-order harmonic, the intensity of the driving laser field usually greatly exceeds that of the emitted harmonic field, making it difficult to observe the effect of VQF on the first-order harmonic amplitude. To mitigate the influence of the intense driving laser field on the emitted harmonic photons and to facilitate a clearer observation of the vacuum squeezing effect on harmonic emission, we can use two crossing driving beams to generate noncollinear HHG, as demonstrated previously [44,45]. In this case, the driving light and the harmonic propagate in different directions and thus do not overlap each other in space.

IV. CONCLUSIONS AND OUTLOOK

We have studied HHG from intense laser-atom interaction in a squeezed vacuum of a single harmonic mode. An analytical formula of the harmonic amplitude in the presence of the squeezed vacuum is derived by employing a fully quantum TDSE. The simulated HHG spectra with the formula show that the harmonic amplitude of the corresponding squeezed mode is influenced by the squeezed vacuum. By using time-frequency analysis, we have elucidated that the quantum fluctuation of the squeezed vacuum affects the probability of the electron transition associated with the harmonic photon emission in squeezed mode, during the rescattered electron recombination with the atomic core. Thus, the amplitude of the harmonic photon is changed accordingly. This finding is consistent with the explanation of Fermi's golden rule. Therefore, our work establishes a direct and fundamental connection between HHG and vacuum fluctuations, offering an unconventional approach to control harmonic generation. Considering the universality of VQF effect on the electron transition, we expect that the effect of VQF can be applied to other atomic emission processes, such as strong-field terahertz radiation.

ACKNOWLEDGMENTS

This work was supported by the National Key Program for S&T Research and Development (No. 2019YFA0307702), the National Natural Science Foundation of China (No. 12121004, No. 12274420, and No. 11922413), and CAS Project for Young Scientists in Basic Research (No. YSBR-055).

S.J.W. and S.G.Y. contributed equally to this work.

[1] M. Ferray, A. L'Huillier, X. F. Li, L. A. Lompré, G. Mainfray, and C. Manus, Multiple-harmonic conversion of 1064 nm radiation in rare gases, J. Phys. B **21**, L31 (1988).

[2] E. A. Gibson, A. Paul, N. Wagner, R. Tobey, S. Backus, I. P. Christov, M. M. Murnane, and H. C. Kapteyn, High-order harmonic generation up to 250 eV from highly ionized argon, Phys. Rev. Lett. **92**, 033001 (2004).

[3] J.-F. Hergott, M. Kovacev, H. Merdji, C. Hubert, Y. Mairesse, E. Jean, P. Breger, P. Agostini, B. Carré, and P. Salières, Extreme-ultraviolet high-order harmonic pulses in the microjoule range, Phys. Rev. A **66**, 021801(R) (2002).

[4] E. Constant, D. Garzella, P. Breger, E. Mével, C. Dorrer, C. Le Blanc, F. Salin, and P. Agostini, Optimizing high harmonic generation in absorbing gases: Model and experiment, Phys. Rev. Lett. **82**, 1668 (1999).

[5] J. Itatani, J. Levesque, D. Zeidler, H. Niikura, H. Pepin, J. C. Kieffer, P. B. Corkum, and D. M. Villeneuve, Tomographic imaging of molecular orbitals, Nature (London) **432**, 867 (2004).

[6] O. Smirnova, Y. Mairesse, S. Patchkovskii, N. Dudovich, D. Villeneuve, P. Corkum, and M. Y. Ivanov, High harmonic interferometry of multi-electron dynamics in molecules, Nature (London) **460**, 972 (2009).

[7] P. M. Paule, E. S. Toma, P. Bregerg, G. Mullot, F. Augé, P. Balcou, H. G. Muller, and P. Agostini, Observation of a train of attosecond pulses from high harmonic generation, Science **292**, 1689 (2001).

[8] F. Krausz and M. Ivanov, Attosecond physics, Rev. Mod. Phys. **81**, 163 (2009).

[9] P. Salières, B. Carré, L. Le Déroff, F. Grasbon, G. G. Paulus, H. Walther, R. Kopold, W. Becker, D. B. Milošević, A. Sanpera, and M. Lewenstein, Feynman's path-integral approach for intense-laser-atom interactions, Science **292**, 902 (2001).

[10] D. B. Milošević and F. Ehlotzky, Scattering and reaction processes in powerful laser fields, Adv. At. Mol. Opt. Phys. **49**, 373 (2003).

[11] C. Figueira de Morisson Faria, High-order harmonic generation in diatomic molecules: A quantum-orbit analysis of the interference patterns, Phys. Rev. A **76**, 043407 (2007).

[12] N. Tsatrafyllis, I. K. Kominis, I. A. Gonoskov, and P. Tzallas, High-order harmonics measured by the photon statistics of the infrared driving-field exiting the atomic medium, Nat. Commun. **8**, 15170 (2017).

[13] A. Gorlach, O. Neufeld, N. Rivera, O. Cohen, and I. Kaminer, The quantum-optical nature of high harmonic generation, Nat. Commun. **11**, 4598 (2020).

[14] M. Lewenstein, M. F. Ciappina, E. Pisanty, J. Rivera-Dean, P. Stammer, T. Lamprou, and P. Tzallas, Generation of optical Schrödinger cat states in intense laser-matter interactions, Nat. Phys. **17**, 1104 (2021).

[15] P. Stammer, J. Rivera-Dean, T. Lamprou, E. Pisanty, M. F. Ciappina, P. Tzallas, and M. Lewenstein, High photon number entangled states and coherent state superposition from the extreme ultraviolet to the far infrared, Phys. Rev. Lett. **128**, 123603 (2022).

[16] A. Pizzi, A. Gorlach, N. Rivera, A. Nunnenkamp, and I. Kaminer, Light emission from strongly driven many-body systems, Nat. Phys. **19**, 551 (2023).

[17] M. E. Tzur, M. Birk, A. Gorlach, M. Krúger, I. Kaminer, and O. Cohe, Photon-statistics force in ultrafast electron dynamics, Nat. Photon. **17**, 501 (2023).

[18] A. Gorlach, M. E. Tzur, M. Birk, M. Krüger, N. Rivera, O. Cohen, and I. Kaminer, High-harmonic generation driven by quantum light, Nat. Phys. **19**, 1689 (2023).

[19] P. Stammer, J. Rivera-Dean, A. Maxwell, T. Lamprou, A. Ordóñez, M. F. Ciappina, P. Tzallas, and M. Lewenstein,

Quantum electrodynamics of intense laser-matter interactions: A tool for quantum state engineering, PRX Quantum **4**, 010201 (2023).

[20] P. Stammer, J. Rivera-Dean, A. S. Maxwell, T. Lamprou, J. Argello-Luengo, P. Tzallas, M. F. Ciappina, and M. Lewenstein, Entanglement and squeezing of the optical field modes in high harmonic generation, Phys. Rev. Lett. **132**, 143603 (2024).

[21] A. Rasputnyi, Z. Chen, M. Birk, O. Cohen, I. Kaminer, M. Kruger, D. Seletskiy, M. Chekhova, and F. Tani, High harmonic generation by bright squeezed vacuum, arXiv:2403.15337; S. Lemieux, S. A. Jalil, D. Purschke, N. Boroumand, D. Villeneuve, A. Naumov, T. Brabec, and G. Vampa, Photon bunching in high-harmonic emission controlled by quantum light, arXiv:2404.05474.

[22] P. W. Milonni, *The Quantum Vacuum: An Introduction to Quantum Electrodynamics* (Academic Press, New York, 1993).

[23] F. Appugliese, J. Enkner, G. L. Paravicini-Bagliani, M. Beck, C. Reichl, W. Wegscheider, G. Scalari, C. Ciuti, and J. Faist, Breakdown of topological protection by cavity vacuum fields in the integer quantum Hall effect, Science **375**, 1030 (2022).

[24] P. Lodahl, A. Floris van Driel, I. S. Nikolaev, A. Irman, K. Overgaag, D. Vanmaekelbergh, and W. L. Vos, Controlling the dynamics of spontaneous emission from quantum dots by photonic crystals, Nature (London) **430**, 654 (2004).

[25] P. B. Corkum, Plasma perspective on strong field multiphoton ionization, Phys. Rev. Lett. **71**, 1994 (1993).

[26] M. Lewenstein, P. Balcou, M. Yu. Ivanov, A. L'Huillier and P. B. Corkum, Theory of high-harmonic generation by low-frequency laser fields, Phys. Rev. A **49**, 2117 (1994).

[27] M. O. Scully and M. S. Zubairy, Quantum Optics (Cambridge University Press, New York, 1997).

[28] D. F. Walls, Squeezed states of light, Nature (London) **306**, 141 (1983).

[29] R. Schnabel, Squeezed states of light and their applications in laser interferometers, Phys. Rep. **684**, 1 (2017).

[30] L.-A. Wu, H. J. Kimble, J. L. Hall, and H. Wu, Generation of squeezed states by parametric down conversion, Phys. Rev. Lett. **57**, 2520 (1986).

[31] A. Furusawa, J. L. Sørensen, S. L. Braunstein, C. A. Fuchs, H. J. Kimble, and E. S. Polzik, Unconditional quantum teleportation, Science **282**, 706 (1998).

[32] R. E. Slusher, L. W. Hollberg, B. Yurke, J. C. Mertz, and J. F. Valley, Observation of squeezed states generated by four-wave mixing in an optical cavity, Phys. Rev. Lett. **55**, 2409 (1985).

[33] S. Liu, Y. Lou, and J. Jing, Interference-induced quantum squeezing enhancement in a two-beam phase-sensitive amplifier, Phys. Rev. Lett. **123**, 113602 (2019).

[34] H. Vahlbruch, M. Mehmet, K. Danzmann, and R. Schnabel, Detection of 15 dB squeezed states of light and their application for the absolute calibration of photoelectric quantum efficiency, Phys. Rev. Lett. **117**, 110801 (2016).

[35] C. E. Vollmer, C. Baune, A. Samblowski, T. Eberle, V. Handchen, J. Fiurasek, and R. Schnabel, Quantum up-conversion of squeezed vacuum states from 1550 to 532 nm, Phys. Rev. Lett. **112**, 073602 (2014).

[36] H. Rütz, K.-H. Luo, H. Suche, and C. Silberhorn, Quantum frequency conversion between infrared and ultraviolet, Phys. Rev. Appl. **7**, 024021 (2017).

[37] G. Breitenbach, S. Schiller, and J. Mlynek, Measurement of the quantum states of squeezed light, Nature (London) **387**, 471 (1997).

[38] X. M. Tong and S.-I. Chu, Theoretical study of multiple high-order harmonic generation by intense ultrashort pulsed laser fields: A new generalized pseudospectral time-dependent method, Chem. Phys. **217**, 119 (1997).

[39] L. K. Jeffrey, J. S. Kenneth, and C. K. Kenneth, High-order harmonic generation from atoms and ions in the high intensity regime, Phys. Rev. Lett. **68**, 3535 (1992).

[40] X. Chu and S.-I. Chu, Optimization of high-order harmonic generation by genetic algorithm and wavelet time-frequency analysis of quantum dipole emission, Phys. Rev. A **64**, 021403(R) (2001).

[41] We choose different values of τ for different harmonics to ensure that the mother wavelet function has a narrow temporal distribution compared to the optical period of the driving light and the corresponding wavelet time-frequency profile is smooth.

[42] J. Rivera-Dean, Th. Lamprou, E. Pisanty, P. Stammer, A. F. Ordóñez, A. S. Maxwell, M. F. Ciappina, M. Lewenstein, and P. Tzallas, Strong laser fields and their power to generate controllable high-photon-number coherent-state superpositions, Phys. Rev. A **105**, 033714 (2022).

[43] P. Lodahl, S. Mahmoodian, and S. Stobbe, Interfacing single photons and single quantum dots with photonic nanostructures, Rev. Mod. Phys. **87**, 347 (2015).

[44] J. B. Bertrand, H. J. Wörner, H.-C. Bandulet, É. Bisson, M. Spanner, J.-C. Kieffer, D. M. Villeneuve, and P. B. Corkum, Ultrahigh-order wave mixing in noncollinear high harmonic generation, Phys. Rev. Lett. **106**, 023001 (2011).

[45] D. D. Hickstein, F. J. Dollar, P. Grychtol, J. L. Ellis, R. Knut, C. Hernández-García, D. Zusin, C. Gentry, J. M. Shaw, T. Fan, K. M. Dorney, A. Becker, A. Jaron-Becker, H. C. Kapteyn, M. M. Murnane, and C. G. Durfee, Non-collinear generation of angularly isolated circularly polarized high harmonics, Nat. Photon. **9**, 743 (2015).